

Naval Research Laboratory

Washington, DC 20375-5320



NRL/MR/6750--99-8382

Measurement of a Planar Discharge and Its Interaction With a Neutral Background Gas

J.A. GREGOR

*Johns Hopkins Applied Physics Laboratory
Laurel, Maryland*

R.F. FERNSLER

R.A. MEGER

*Charged Particle Physics Branch
Plasma Physics Division*

June 25, 1999

19990629 056

Approved for public release; distribution is unlimited.

REPORT DOCUMENTATION PAGE

Form Approved
OMB No. 0704-0188

Public reporting burden for this collection of information is estimated to average 1 hour per response, including the time for reviewing instructions, searching existing data sources, gathering and maintaining the data needed, and completing and reviewing the collection of information. Send comments regarding this burden estimate or any other aspect of this collection of information, including suggestions for reducing this burden, to Washington Headquarters Services, Directorate for Information Operations and Reports, 1215 Jefferson Davis Highway, Suite 1204, Arlington, VA 22202-4302, and to the Office of Management and Budget, Paperwork Reduction Project (0704-0188), Washington, DC 20503.

1. AGENCY USE ONLY (Leave Blank)	2. REPORT DATE	3. REPORT TYPE AND DATES COVERED	
	June 25, 1999	Interim	
4. TITLE AND SUBTITLE Measurement of a Planar Discharge and Its Interaction With a Neutral Background Gas			5. FUNDING NUMBERS 67-7641-A9
6. AUTHOR(S) J.A. Gregor,* R.F. Farnsler, and R.A. Meger			
7. PERFORMING ORGANIZATION NAME(S) AND ADDRESS(ES) Naval Research Laboratory Washington, DC 20375-5320			8. PERFORMING ORGANIZATION REPORT NUMBER NRL/MR/6750-99-8382
9. SPONSORING/MONITORING AGENCY NAME(S) AND ADDRESS(ES) Office of Naval Research 800 North Quincy Street Arlington, VA 22217-5660			10. SPONSORING/MONITORING AGENCY REPORT NUMBER
11. SUPPLEMENTARY NOTES * Johns Hopkins Applied Physics Laboratory Laurel, MD			
12a. DISTRIBUTION/AVAILABILITY STATEMENT Approved for public release; distribution unlimited.			12b. DISTRIBUTION CODE
13. ABSTRACT (Maximum 200 words) The effect of a weakly ionized glow discharge plasma on the temperature and density of a neutral background gas has been investigated. The particular discharge studied is a magnetically confined $50\text{ cm} \times 60\text{ cm} \times 3\text{ cm}$ planar sheet plasma produced using the Agile Mirror system at the U.S. Naval Research Laboratory. Most previous glow discharge work has concentrated on either the DC characteristics, or on the very early evolution ($< 1 - 2\text{ }\mu\text{s}$) of the discharge. This paper analyzes the results of time-resolved measurements made over intermediate ($5 - 300\text{ }\mu\text{s}$) timescales. Measurements made of an air discharge produced using $V_D = 4.5\text{ kV}$ anode-cathode voltage, $P_N \sim 120\text{ mTorr}$ background gas pressure, and $B = 250\text{ G}$ external magnetic field reveal an $n_e = 10^{12}\text{ cm}^{-3}$, $T_e = 1\text{ eV}$ negative glow plasma. Measurements made on an air discharge produced using $V_D \sim 2-3\text{ kV}$, $P_N \sim 208\text{ mTorr}$, and $B \sim 250\text{ G}$ reveal an $n_e = 10^{11}\text{ cm}^{-3}$, $T_e = 1-3\text{ eV}$ plasma with distinct negative glow, Faraday dark space, and positive column regions. Analysis of time-resolved potential, temperature, and spectroscopic data reveal that the higher pressure discharge transitions after $\sim 100\text{ }\mu\text{s}$ into a homogeneous negative glow discharge. Quantitative analysis of the discharge taking into account the important ionization and loss processes, and using measurements of discharge current, voltage, and local electric field, confirms that a $>50\%$ reduction in neutral gas density due to heating of the background gas is responsible for the transition.			
14. SUBJECT TERMS			15. NUMBER OF PAGES 32
			16. PRICE CODE
17. SECURITY CLASSIFICATION OF REPORT UNCLASSIFIED	18. SECURITY CLASSIFICATION OF THIS PAGE UNCLASSIFIED	19. SECURITY CLASSIFICATION OF ABSTRACT UNCLASSIFIED	20. LIMITATION OF ABSTRACT UL

CONTENTS

Abstract	1
I. Introduction	2
II. Glow Discharge Formation	2
III. The Experiment	5
A. Agile Mirror Apparatus	5
B. Diagnostics	5
IV. Experimental Results	6
A. Optical Emission Measurement	7
B. Floating Probe Measurements	8
C. Plasma Density Measurements	9
D. Plasma Temperature Measurement	10
V. Analysis of Experimental Results	11
A. Cathode Effects	11
B. Beam Density in the NG-only and PC/NG	12
C. Gas Heating in the Positive Column	14
D. Gas Heating in the Negative Glow of the PC/NG Discharge	15
E. Channel Density and Beam Range	15
F. Self-consistent Calculation of Channel Density	17
VI. Conclusions	19
Acknowledgements	20
References	21
Figures	22-29

Measurement of a Planar Discharge and Its Interaction With a Neutral Background Gas

J. A. Gregor,^a R. F. Farnsler, R. A. Meger

Plasma Physics Division
Naval Research Laboratory
Washington, DC 20375-5346

Abstract

The effect of a weakly ionized glow discharge plasma on the temperature and density of a neutral background gas has been investigated. The particular discharge studied is a magnetically confined 50 cm x 60 cm x 3 cm planar sheet plasma produced using the Agile Mirror system at the U.S. Naval Research Laboratory. Most previous glow discharge work has concentrated on either the DC characteristics, or on the very early evolution (< 1 - 2 μ s) of the discharge. This paper analyzes the results of time-resolved measurements made over intermediate (5 - 300 μ s) timescales. Measurements made of an air discharge produced using a $V_D = 4.5$ kV anode-cathode voltage, $P_N \approx 120$ mTorr background gas pressure, and $B = 250$ G external magnetic field reveal an $n_e = 10^{12}$ cm⁻³, $T_e = 1$ eV negative glow plasma. Measurements made on an air discharge produced using $V_D \approx 2-3$ kV, $P_N \approx 208$ mTorr, and $B \approx 250$ G reveal an $n_e = 10^{11}$ cm⁻³, $T_e = 1-3$ eV plasma with distinct negative glow, Faraday dark space, and positive column regions. Analysis of time-resolved potential, temperature, and spectroscopic data reveal that the higher pressure discharge transitions after ≈ 100 μ s into a homogeneous negative glow discharge. Quantitative analysis of the discharge taking into account the important ionization and loss processes, and using measurements of discharge current, voltage, and local electric field, confirms that a > 50% reduction in neutral gas density due to heating of the background gas is responsible for the transition.

^a Work Supported by the Office of Naval Research

^a Present Address: Johns Hopkins Applied Physics Lab, Laurel, MD 20723
Manuscript approved June 7, 1999.

I. Introduction

In this paper we investigate the properties of a hollow-cathode produced glow discharge plasma employed in a new type of microwave beam steering antenna called the Agile Mirror.^{1,2,3,4,5} The goal of the Agile Mirror program is to create a stable plasma sheet capable of reflecting x-band microwaves over 0.1-10.0 ms timescales. This paper investigates the influence of discharge voltage and neutral gas density on the formation and time evolution of the plasma sheet. Observed effects were particularly strong for higher neutral gas density and lower driver voltages, which produced lower density plasma sheets with time dependent characteristics. In order to investigate these effects, measurements of plasma temperature, density, and local electric field were made on a discharge generated in a high density background gas. These measurements were compared with similar data obtained from a lower pressure, higher voltage discharge. The results provide insight into the formation of the plasma and indicate that heating of the background gas plays a significant role in the formation and time evolution of the discharge.

II. Glow Discharge Formation

A glow discharge is commonly produced by impressing high voltage across two electrodes immersed in a low pressure gas. The naturally occurring background ionization of the neutral gas leads to a current flow between the electrodes. A plasma sheath forms near the cathode. Positively charged ions from this sheath are accelerated onto the cathode surface, liberating electrons via secondary emission. The emitted electrons are in turn accelerated into the discharge channel, ionizing the background gas and sustaining the discharge. Once initiated, the voltage gradients and plasma densities within the discharge channel adjust themselves to maintain the discharge. The ionization mechanism for generating and sustaining the plasma may change locally, but the total current flowing through the plasma must be continuous at all points between the anode and cathode. Two distinctly different types of discharges may be formed in this way. In one type, referred to as a negative glow (NG), the plasma is maintained via impact ionization from high energy electrons from the cathode surface. In the other type,

referred to as a positive column (PC), the plasma is maintained locally via avalanche ionization.

In the NG type discharge, electrons leave the hollow cathode with an energy $W \approx eV_D$, where V_D is the voltage across the discharge. These electrons have a long mean free path and leave behind a trail of ionization as they propagate from cathode to anode. Beam induced ionization is relatively efficient, producing a cold, high density plasma. Internal electric fields of $E \ll 1$ V/cm and plasma densities of $\approx 5 \times 10^{12}$ cm⁻³ are typical⁴ while the discharge current is carried by a combination of beam electrons and bulk plasma current. The ultimate length of the NG is set by the energy loss range of the cathode-produced beam electrons. For high electron energies and low gas densities the NG can extend across the entire length of the anode-cathode (A-K) gap.

For beam ranges shorter than the A-K gap, current continuity requires that another form of ionization generate sufficient plasma density to maintain the discharge current. In this case the electric field in the discharge channel adjusts itself until it can accelerate plasma electrons sufficiently to ionize the background gas. The field necessary to sustain a discharge in this way depends on the gas density, gas species, and discharge current. Only a small fraction of the plasma electrons need reach energies high enough to ionize the background gas. The majority are accelerated by the field but lose their energy to collisions with the background before they can gain enough energy to ionize neutrals. These collisions heat and excite the neutral gas. This type of discharge is called a positive column (PC) and the process sustaining the discharge is called avalanche ionization. The avalanche ionization process is far less efficient than beam ionization and produces a higher temperature, lower density plasma. The PC is characterized by a normalized electric field of $E/P \approx 35$ V/cm-Torr^{6,7} and plasma densities a factor of 5-10 times lower than those found in a comparable NG discharge.

In the Agile Mirror a linear hollow cathode and uniform DC magnetic field are used to generate a planar high voltage electron beam. The hollow cathode is formed from brass "U" channel 1.2 cm wide by 1 cm deep by 50 cm long. This cathode produces an approximately 2 cm thick (FWHM) by 50 cm wide discharge within the A-K gap when pulsed by a 1.5-7 kV square-wave voltage generator.⁸ The voltage pulse drives 5-30 amps through the discharge, of which only a fraction is electron beam

current. An electron energy analyzer⁹ placed behind the anode showed a relatively wide energy distribution function for the beam electrons with a peak at $\sim 0.7 \times V_0$. The FWHM of the distribution function was $\sim 0.5 \times V_0$ with electrons ranging from full voltage down to zero. A plasma is formed as these beam electrons collide with neutral gas molecules and ionize the background gas. Ions within the plasma are accelerated toward the cathode, where they interact within the hollow cathode region to produce additional beam electrons via secondary electron emission. The plasma discharge and cathode operate in an equilibrium determined by the properties of the gas, cathode shape and surface properties, and the load line of the HV supply. An external 150-300 Gauss magnetic field connecting the cathode to the anode confines the beam electrons laterally so that the resulting plasma forms a well defined sheet, 50 cm wide by 60 cm long and ≈ 2 cm FWHM thick. High voltage ($V_D > 4.5$ kV), low pressure ($P_N < 150$ mTorr), operation produces a NG-type plasma that extends across the entire A-K gap. This discharge is capable of reflecting 10 GHz microwaves with characteristics comparable to that of a flat metal plate.^{3,4} If the voltage is decreased ($V \leq 3$ kV) and the background pressure increased ($P > 150$ mTorr) a PC type plasma appears at the anode end of the discharge. Visually, the discharge appears to be composed of two well defined regions, NG-type near the cathode and PC-type near the anode. The relative size of the two regions depends on the neutral gas density and discharge voltage. This parameter regime produces a lower density plasma which does not reflect X-band microwaves. Time resolved measurements indicate that the size of the PC actually changes during the life of the discharge. The PC, initially established over 1/3 to 1/2 of the discharge length, transitions after 100-200 μ s into a NG. A detailed study of this transition provides insight into the interaction between the cathode emitted beam electrons and the background gas. To this end time-resolved measurements of the electron temperature, density, electric field, and optical emission from the plasma were made in both the NG-only and PC/NG discharges. The results suggest that heating of the background gas plays a key role in discharge evolution. Quantitative analysis indicates that the gas density drops by $\sim 50\%$ during the first 150 μ s of the discharge, resulting in the transition from a PC/NG discharge to a NG-only discharge.

III. The Experiment

A. Agile Mirror Apparatus:

The Agile Mirror apparatus (see Fig. 1) consists of a cylindrical acrylic vacuum chamber, 79 cm in diameter and 81 cm long. The chamber is centered within a Helmholtz coil pair capable of producing a 500 Gauss DC magnetic field with a uniformity better than 1% over the volume of interest. Spectroscopic and microwave diagnostics have access to the plasma through the acrylic sidewalls of the chamber. Vacuum ports in the end plates provide access for pumping, probes, and other diagnostics.

The linear hollow cathode is suspended from the center of the top endplate. A thin 58 cm diameter brass disk supported by the bottom endplate serves as the anode. The chamber is first evacuated to a base pressure < 20 mTorr using a mechanical roughing pump, then the operating pressure is set via an adjustable leak valve. The fill gas (ambient air in the experiments reported here) is exchanged approximately every 15 s. The discharge was operated in a pulsed mode using ≈ 300 μ s long HV pulses triggered at a ≈ 1 Hz rate. An $80\text{-}\Omega$ series ballast resistor connected the power supply to the Agile Mirror cathode and determined the load-line for the driver. Discharge current was provided by a $60\text{ }\mu\text{f}$ reservoir capacitor. HV was applied to the cathode via a Crossatron-based⁸ modulator system capable of switching times on the order of 100-200 ns with ± 5 ns jitter. The discharge voltage differs from the bank charging voltage V_0 by the voltage drop across the Crossatron switch (fixed at ≈ 500 V) and the series ballast resistor.

B. Diagnostics:

Discharge voltage V_D was measured using a parallel high impedance shunt and calibrated Rogowski current monitor. Discharge current I_D was measured using another Rogowski current monitor sensing the total current passing through the anode to ground. Voltage and current measurements were time resolved to better than 1 μ s.

The axial electric field $E_z(z,t)$ within the plasma was derived from floating potential $V_f(z,t)$ measurements made by inserting an unbiased probe into the plasma.

The impedance of the probe was made finite by design in order to obtain response times $<2 \mu\text{s}$. As a result the measured potential deviated from the true floating potential V_f by a constant 4 - 5 V. This does not affect the electric field calculation. V_f measurements were averaged over five discharge pulses to improve the signal-to-noise ratio and reduce the effects of shot-to-shot variation.

Langmuir probes, supplemented by microwave diagnostics, were used to measure the plasma electron density n_e and temperature T_e within the discharge. These probes were constructed from rigid coaxial cable capped with castable ceramic housing a single sided planar copper collector with area $\approx 1.8 \text{ mm}^2$. Exposed non-collecting areas were insulated with Formvar. In this experiment the plasma electrons were magnetized with Larmor radii $r_{Le} \approx \delta/5$ where δ is the linear dimension of the probe while the ions were essentially unmagnetized with $r_{Li} \approx 5\delta$. Measurements were made with the probe's collection area oriented both perpendicular and parallel to the magnetic field. Change of the probe orientation relative to the magnetic field did not appear to make a significant difference to the measured signal. Probe data at each spatial location was averaged over 12 discharge pulses in order to improve the signal to noise ratio and reduce the effects of shot-to-shot variation.

Spectroscopic measurements were used to track the time-resolved behavior of the PC region in the PC/NG discharge. The relative amplitude of the brightest lines in the visible were measured using a photomultiplier connected to a Spex 1702 monochromator equipped with a 1200 line grating.

IV. Experimental Results

Baseline measurements were made using a 6.5 kV charging voltage, 300 μs long pulse, 120 mTorr air gas fill, and 250 Gauss magnetic field. This set of parameters produced a uniform 50 cm x 60 cm, high density ($n_e > 10^{12} \text{ cm}^{-3}$), NG-only plasma sheet for the duration of the HV pulse. Figure 2 shows the discharge voltage and current waveforms for this case. The difference between the charging voltage V_0 and the discharge voltage V_D represents the voltage drops across the Crossatron and the 80 Ω ballast resistor. The discharge voltage initially drops by $\approx 10\%$, then slowly rises to a level 10% above its initial magnitude. The discharge current I_D peaks when V_D is at a

minimum, then falls to \approx 60% of its peak magnitude. After the initial variation I_D and V_D remain nearly constant for pulses lasting several milliseconds.

For the PC/NG case, data was taken using V_0 = 2.0, 2.5, and 3.0 kV with a pulse length of 300 μ s. The fill gas was air at $P_N \approx$ 208 mTorr and the magnetic field was B = 250 Gauss. Figures 3a and 3b show the voltage and current traces for the PC/NG discharge. In this case the voltage initially drops by \approx 25% independent of driver voltage, later recovering to a level \approx 25% above its initial magnitude. The discharge current is again high during the first 100 μ s before falling to \approx 20% of its initial magnitude in equilibrium. The excursions in I_D and V_D for the PC/NG discharge match in character those observed in the NG-only discharge, but are more exaggerated in magnitude.

A. Optical Emission Measurement:

One of the most striking differences between the NG-only and PC/NG discharges is in their visible light emissions.^{10,11} Using air as the fill gas we observe a high density NG-only plasma which appears bluish-white to the naked eye. As the voltage is lowered and the fill gas pressure increased, the emissions near the cathode region shifts toward the blue, while those near the anode region become red-orange. The blue and orange regions are separated by a short region which emits very little light. These emissions are typical of glow discharges formed in N_2 or air, where the blue-white region corresponds to a NG-type discharge, the orange region corresponds to a PC-type discharge, and the dark region connecting the two is called the Faraday Dark Space (FDS).¹¹ During a single pulse the naked eye sees a plasma with fixed NG, FDS, and PC regions. Time resolved measurement of light emissions from the PC/NG discharge (V_0 = 3 kV) indicate, however, that the region near the anode changes from a PC-type plasma to a NG-type plasma after \approx 150 μ s. The four brightest lines in the (uncalibrated) 400-700 nm range were recorded using a photomultiplier tube (see Fig. 4). Peaks were centered about 416 (violet), 459 (blue), 626 (orange), and 677 nm (red). Emission in three of the lines dropped to very low levels after 100-120 μ s. The fourth displayed a rapidly decreasing signal early in time, followed by a momentary peak centered at \approx 135 μ s, and ending with a slow increase to an equilibrium level by the end of the HV discharge pulse. The emissions early in time, during the PC phase of the discharge, are

dominated by red/orange line radiation, while emissions late in time are primarily near the blue 459 nm peak. This correlates with electric field measurements made near the position being imaged, which indicate a transition from a PC-type to a NG-type plasma approximately 100-135 μ s into the discharge pulse. The momentary increase in 459 nm emissions at 140 μ s suggests that some process is maximized within the spectrometer field of view (centered about a position \approx 42 cm from the cathode) at that time.

B. Floating Probe Measurements:

A high impedance probe positioned at the plasma at the peak of the plasma density distribution was used to measure the local floating potential relative to ground. Measurements of the local floating potential made at various positions along the length of the plasma were used to map out V_f as a function of distance from the cathode. Individual measurements (made on a shot-to-shot basis) were highly reproducible, thus allowing spatial measurements to be taken over a period spanning several thousand pulses. The data was averaged over multiple pulses in order to improve the signal-to-noise ratio and to reduce the effects of shot-to-shot variation. The local electric field, $E_z(z, t)$, was obtained by taking the spatial derivative of $V_f(z, t)$.

For the NG-only case shown in Fig. 5a the floating potential 25 μ s into the pulse decreased smoothly with distance from \approx -13 V at a position 10 cm from the cathode to \approx -8 V near the anode (55 cm from the cathode). This corresponds to a longitudinal electric field of \approx 0.1 V/cm within the plasma. Calculations show that a normalized electric field strength of $E/P > 35$ V/cm-Torr or equivalently $E/N > 1\times 10^{-15}$ V-cm² is required to sustain an avalanche discharge in air with density N cm⁻³. This corresponds to $E > 4$ V/cm for 120 mtorr air,⁷ much higher than the field measured in the NG-only discharge, indicating that the plasma is being maintained by a non-local source of ionization. Figure 5a also shows the electric field decreasing with time for the duration of the HV pulse, indicating that conditions within the neutral background gas itself are changing.

The PC/NG case shown in Fig. 5b is markedly different. There appear to be two distinct regions of space charge potential along the plasma sheet which collapse into a single region after \approx 100 μ s. Near the cathode the space charge potential initially

exceeds -200 V relative to the anode, increases to -270 V after 60 μ s, then rapidly drops to -50 V after 130 μ s. The electric field in this region is initially \approx 0.1 V/cm 5 μ s into the pulse, increases to \approx 0.3 V/cm after 60 μ s, and finally settles down to \approx 0.35 V/cm after 130 μ s. Excluding the cathode fall, most of the potential drop across the discharge appears across the PC region, near the anode. This region contains a relatively constant electric field of $E_z \approx$ 7.5 V/cm. After 130 μ s E_z drops to a nearly uniform \approx 0.35 V/cm over the entire length of the discharge. Figure 6 illustrates the change in electric field strength 35 cm from the cathode as a function of time for three different discharge voltages. Note that the electric field early in time is essentially independent of V_0 . E_z decreases as a function of time from \approx 8 V/cm down to \approx 5 V/cm after 75 μ s, then rapidly drops to \approx 0.3 V/cm after a time period that depends on V_0 . This final transition appears to take place at \approx 155 μ s, 115 μ s, and 95 μ s, for the V_0 = 2.0, 2.5, and 3.0 kV cases respectively. This suggests that the character of the plasma discharge changes after \approx 75-150 μ s, depending on the discharge charge voltage. Early in time the region near the cathode supports a NG-type plasma with $E_z < 0.3$ V/cm. In the region near the anode the initial electric field is much higher, with $E_z \approx$ 8 V/cm, which agrees well with the voltage necessary to maintain an avalanche discharge in 208 mTorr air. This field decreases gradually over the next 75-150 μ s to \approx 4 V/cm before dropping rapidly to \approx 0.3 V/cm, a level indicative of a non-locally supported NG-type plasma.

C. Plasma Density Measurements:

Plasma density measurements were made in both the baseline NG-only and the PC/NG discharges using microwave transmission and Langmuir probe diagnostics. The NG-only discharge achieved cutoff for a 10 GHz CW signal propagating perpendicular to the sheet indicating a plasma density $n_e \geq 1.2 \times 10^{12}$ cm⁻³. The PC/NG discharge, produced under identical conditions, did not reach cutoff density; indicating a plasma density $n_e < 1.2 \times 10^{12}$ cm⁻³ for this case.

Electric probes were used to obtain an independent measurement of the plasma density. For a given set of plasma parameters (V_D , P_N , and B), probe current was measured while holding the probe at a fixed bias with respect to the anode. V_D , P_N , and B changed less than 10% during data collection and were highly reproducible from shot-

to-shot. Time-resolved Langmuir curves for the plasma were constructed using data collected while varying the probe bias from electron saturation to ion saturation on a shot-to-shot basis. An example is illustrated in Fig. 7. This figure shows curves for a NG-only discharge 42 cm from the cathode. Traces are shown for data using three different probe orientations: toward the cathode, toward the anode, and perpendicular to the anode-cathode axis. Similar probe characteristic traces were taken from the PC/NG case. In this case the 42 cm probe location fell within the early time PC portion of the discharge.

Langmuir probe measurements were not taken during the PC phase of the PC/NG discharge, due to the ~ 250 V change in the local floating potential associated with the transition to a NG discharge. To protect the probe driver electronics, a triggered switch was used to isolate the probe during the initial $150 \mu\text{s}$ period when the PC was present. Once conditions within the discharge had settled, the probe was connected to the bias network, enabling measurements to be made during the later NG phase of the discharge. Figure 8 shows n_e ($t > 150\mu\text{s}$) derived from ion saturation current measurements of both the baseline NG-only discharge and the PC/NG discharge with $V_0 = 3$ kV. The probe in the NG-only discharge yielded $n_e \approx 8.5 \times 10^{11} \text{ cm}^{-3}$ in equilibrium. While somewhat below the density inferred from microwave measurements, this is well within experimental error given uncertainties in probe area, probe alignment, and magnetic field effects. The PC/NG discharge yielded a smaller $n_e \approx 1.2 \times 10^{11} \text{ cm}^{-3}$ measured after the transition to a NG discharge.

D. Plasma Temperature Measurement:

Electron temperature T_e [eV] was obtained from the probe characteristic by fitting the data near V_f to an assumed Maxwellian plasma distribution:

$$I = I_{is} + I_{es} e^{-e(V_p - V_B)/T_e} \quad (1)$$

where I_{is} is the ion saturation current, I_{es} is the electron saturation current, V_p is the plasma potential and V_B is the probe bias. A curve fitting routine is used to solve for the electron temperature T_e . Figure 9 shows the electron temperature as a function of time for the NG-only discharge and for the NG phase of the PC/NG discharge with $V_c = 3$ kV.

The baseline NG-only discharge showed the bulk of the electron distribution falling within the 1 - 1.5 eV range. There is evidence of a small but distinct component in the 4 - 6 eV range as well. T_e settles to a constant 1.5 eV during the NG phase of the PC/NG distribution.

V. Analysis of Experimental Results

Experimental measurements suggest that the discharge is in local equilibrium at any given time and position, but that the equilibrium changes as a function of time during the pulse. Indications are that both the electron source and the local gas density are changing with time during the discharge pulse, and that the combination of the two leads to the observed transition from a PC/NG to a pure NG discharge late in time.

A. Cathode Effects:

No direct measurements were made of the beam current density or electron energy produced by the hollow cathode. The voltage between the cathode and anode, the total current through the discharge, and the electric field within the plasma sheet, however, were measured. Beam electrons gain their energy crossing the sheath near the cathode surface. This sheath voltage adjusts itself to be consistent with the voltage drop across the rest of the discharge and the driver voltage. The measured voltage gradient in the NG portion near the cathode is <0.5 V/cm while the gradient in the PC region is 4-8 V/cm. Thus the total voltage drop from the cathode sheath to the anode is <300 V (see Fig. 5b) and most of the discharge voltage appears across the cathode sheath. Thus the operation of the circuit is dominated by the cathode rather than the NG and PC regions of the discharge. A change in the cathode impedance will significantly affect the operation of the system. Figure 3 illustrates this effect. Early in time the cathode operates at ~ 130 Ω impedance. After 100-150 μ s the impedance jumps to ~ 1000 Ω . This rapid change in diode impedance is most likely due to gas heating inside of the hollow cathode. The scope of this study did not extend to details of the diode operation. The observed change in the discharge from a PC/NG to a NG-only discharge was enhanced by the coincident changes in diode operation, but the *nature* of the discharge equilibrium (ionization vs losses) remains unaffected.

B. Beam Density in the NG-only and PC/NG:

Plasma electron density measurements made during the negative glow phase of the discharge can be used to infer the beam current density, assuming an equilibrium between plasma production due to beam ionization and losses due (primarily) to two-body recombination. A quantitative estimate of plasma production may be obtained by calculating the amount of beam energy deposited in the gas in the form of ionization. The beam energy loss per unit axial length depends on the background neutral gas pressure P_N [Torr] (or equivalently the neutral density N [cm⁻³]) and the electron energy W [eV] according to the following equations

$$\frac{dW}{dz} \approx 2.4 \times 10^5 \frac{P_N}{W} = 6.7 \times 10^{-12} \frac{N}{W} \quad [\text{eV/cm}] \quad (2)$$

where z represents the distance along a line from the cathode to anode.^{5,12} The coefficients for the above equations assume an average impact parameter for the 1.5 - 3 kV electron energies used in the experiment and a 10% decreased path length due to the helical electron orbits (a result of propagation in a magnetic field). As discussed earlier, the electron energy is assumed to be $W \approx 0.7 V_c$ allowing for the measured energy distribution of the beam electrons. The beam induced ionization rate depends on beam flux, j_b/e , and the energy loss, W_{ei} , per electron-ion (e-i) pair produced. For beam energies of several hundred eV or more in air, $W_{ei} \approx 34$ eV and the volumetric ionization rate is

$$\frac{dn_e}{dt} \approx \frac{j_b}{e} \frac{dW}{dz} \left(\frac{1}{W_{ei}} \right). \quad [\text{s}^{-1}] \quad (3)$$

Plasma production is balanced by recombination and diffusion. For a high density ($n_e > 10^{12}$ cm⁻³) beam produced plasma, two-body recombination is the dominant loss mechanism, giving a loss rate of

$$\frac{dn_e}{dt} \approx -\beta n_e^2 \quad [\text{s}^{-1}] \quad (4)$$

where $\beta \approx 5 \times 10^{-8}$ cm⁶/s is the recombination coefficient for cold electrons in weakly ionized air.¹³ Equating (3) and (4) and solving for j_b gives the beam current density as a function of the measured plasma density,

$$j_b = 1.1 \times 10^{-30} n_e^2 \frac{W}{P_N} = 3.9 \times 10^{-13} n_e^2 \frac{W}{N} \quad [A/cm^2] \quad (5)$$

This equation can be applied to the NG-only case shown in figure 1. The discharge current (beam plus plasma current) at $t = 20 \mu s$ was 27 A and the voltage across the discharge was 3.6 kV. The negative glow region encompasses the entire discharge in this case so the cathode voltage is essentially the discharge voltage and $W \approx 0.7 \times V_c \approx 2.5 \text{ kV}$. This early in the pulse, the background gas has not had time to respond to beam heating so the neutral density in the discharge channel is still close to the initial density ($N \approx 4.3 \times 10^{15} \text{ cm}^{-3}$ for $P_N = 120 \text{ mTorr}$). From Fig. 7 the electron density at $t=20 \mu s$ for the NG-only case is $n_e \approx 1.8 \times 10^{12} \text{ cm}^{-3}$. Equation (5) predicts a beam current density of $j_b \approx 75 \text{ mA/cm}^2$ under these conditions. The hollow cathode source has a $1.2 \text{ cm} \times 50 \text{ cm}$ aperture, giving an average discharge current density of $j_d \approx 450 \text{ mA/cm}^2$ for the cathode including both the beam and plasma current j_p . Beam electrons are produced in the hollow cathode via secondary emission as a result of ion bombardment of the cathode surface, and by ionization of neutrals within the sheath by the resultant secondary electrons. Current at the immediate surface of the cathode is carried primarily by the ions striking the cathode. In the body of the discharge the plasma current is carried by low energy plasma electrons. The ratio of the beam density to the plasma current density at the aperture of the cathode represents an effective secondary emission coefficient¹⁴ γ_{eff} for the cathode. For the NG beam $\gamma_{eff} = j_b/(j_d - j_b) \approx 75/(450-75) = 0.2$. The actual secondary emission coefficient will depend on cathode material, ion energy, and other parameters. The value $\gamma_{eff} \approx 0.2$ is not unreasonable at ion energies of several keV.

A similar calculation may be done for the PC/NG discharge at $t = 160 \mu s$, after the plasma has transitioned to a pure NG. For the 3-kV case shown in figure 3 the discharge voltage and current are 2.1 kV and 3.2 A at $160 \mu s$. The average discharge current density is $j_d \approx 53 \text{ mA/cm}^2$ versus 450 mA/cm^2 for the NG-only case. Langmuir probe measurements yield $n_e \approx 1.0 \times 10^{11} \text{ cm}^{-3}$ at $160 \mu s$. Assuming $N \approx 4.6 \times 10^{15} \text{ cm}^{-3}$ (the same as measured at the end of the PC phase - see following section) and a mean electron energy of 1.5 keV equation (5) predicts a beam current density of $j_b \approx 0.13$

mA/cm^2 - nearly a factor of 600 smaller than the NG-only case. The secondary emission coefficient in this case is $\gamma_{\text{eff}} \approx 2.4 \times 10^{-3}$ - two orders of magnitude lower than for the higher voltage NG-only case. This indicates that far fewer high-energy electrons escape from the hollow cathode in this parameter regime. These data indicate that the operation of the hollow cathode is changing with time during the discharge pulse.

C. Gas Heating in the Positive Column:

Figure 6 shows the time history of the local electric field 35 cm from the cathode in the PC/NG discharge. At this distance the probe is within the PC region of the discharge before transition. The electric field early in time, $E_z \approx 7.8 \text{ V/cm}$, did not change with charging potential for the three cases studied ($V_c = 2, 2.5, 3 \text{ kV}$). The initial neutral gas pressure in the chamber was $P_N = 208 \text{ mTorr}$, giving a normalized electric field of $E/P_N \approx 37.5 \text{ V/cm-Torr}$, in good agreement with breakdown field calculations.⁷ Over the next 75-150 μs the electric field for all three cases decreased gradually to 3.5-4.8 V/cm. From this point all three cases appear to follow the same curve, collapsing or transitioning to a lower value at a time determined by V_c . If one assumes that the discharge always operates at the breakdown limit, the electric field gives the density as a function of time in the channel. The data indicates that the neutral gas density within the discharge channel at the time of transition had dropped from an initial $N = 7.4 \times 10^{15} \text{ cm}^{-3}$ to 3.3, 4.3, and $4.6 \times 10^{15} \text{ cm}^{-3}$ for the 2, 2.5, and 3 kV cases respectively.

As an additional check, the plasma current and electric field may be used to calculate the ohmic heating within the discharge. For the 2.5 kV case the average discharge current during the first 100 μs (before transitioning to a NG-only discharge) was $\approx 7 \text{ A}$. The cross sectional area of this plasma sheet was $\approx 100 \text{ cm}^2$ giving an average current density of $J \approx 70 \text{ mA/cm}^2$. The average electric field in the PC portion of the discharge was $E \approx 6 \text{ V/cm}$ during this time period, giving an energy deposition rate of $J_d \times E \approx 0.42 \text{ W/cm}^3$ and a total energy deposition of $W \approx J_d \times E \cdot \Delta t = 42 \times 10^{-6} \text{ J/cm}^3$. If all of the energy ends up as heat in the discharge channel, the temperature would rise by $\Delta T \approx 160 \text{ }^\circ\text{K}$. Assuming constant pressure in the channel, the final neutral

gas density would be $N \approx 4.5 \times 10^{15} \text{ cm}^{-3}$ ($\sim 128 \text{ mTorr}$ equivalent pressure). This is in good agreement with our previous neutral gas density calculation based on the assumption that E/N remains a constant.

D. Gas Heating in the Negative Glow Region of the PC/NG Discharge:

In the PC/NG discharge the plasma near the cathode is generated by high energy electrons from the cathode. Two potential sources of heating are present within the NG, ohmic heating due to the plasma current and energy deposition by the electron beam source. The electric field in this region was $E(\text{NG}) \approx 0.3 \text{ V/cm}$, compared with the $E(\text{PC}) \approx 6 \text{ V/cm}$ measured in the PC region near the anode. Since the discharge current is essentially continuous and $j_b \ll j_d$, ohmic heating of the neutral gas within the NG should be decreased by a factor of $E(\text{NG})/E(\text{PC}) \approx 0.05$. Ohmic heating is thus expected to be relatively small in the NG region.

An estimate of the beam heating rate, R_b , in the NG region can be made by rewriting equation (2) as a function of the discharge current and the beam current fraction γ_{eff} giving

$$R_b = j_b \frac{dW}{dz} \approx 6.7 \times 10^{-12} j_d \left(\frac{\gamma_{\text{eff}}}{1 + \gamma_{\text{eff}}} \right) \frac{N}{W}. \quad [\text{W/cm}^3] \quad (6)$$

At $t=20 \mu\text{s}$ the $V_0 = 2.5 \text{ kV}$ data in figure 3 shows that $V_c = 1.0 \text{ kV}$ and $I_d = 8.0 \text{ A}$. This corresponds to $W = 700 \text{ V}$ and $j_d \approx 130 \text{ mA/cm}^2$, assuming that the beam cross sectional area corresponds to the cathode area. The neutral density is still close to the initial density at $P_N = 208 \text{ mTorr}$. Equation (6) includes the relation $j_b = j_d \gamma_{\text{eff}} / (1 + \gamma_{\text{eff}})$. This gives an energy deposition rate for the beam of $R_b \approx 0.02 \text{ W/cm}^3$ assuming that $\gamma_{\text{eff}} \approx 2.4(-3)$ as found in Section V-B above. This is small compared to the PC discharge heating rate of $\sim 0.4 \text{ W/cm}^3$, indicating that most of the gas heating occurs in the PC portion of the discharge.

E. Channel Density and Beam Range:

The neutral gas density in the NG portion of the PC/NG discharge may also be estimated from beam range measurements made prior to the transition to NG-only.

Equation (2) shows the energy loss rate for the beam electrons. If the range is shorter than the distance from cathode to anode, the beam electrons will eventually slow enough to join the background plasma distribution. The nature of the discharge changes at this point from a beam-sustained NG discharge to an avalanche sustained PC discharge. Since the time taken for the beam electrons to travel from the cathode to the end of their range is short relative to the thermal expansion time of the neutral gas in the channel, the beam electrons pass through what is effectively a static gas distribution. Thus the transition from a NG to a PC defines the range of the beam electrons and thereby provides an estimate of the background gas density in the NG.

Figure 6 shows the measured time dependent electric field at $z = 35$ cm from the cathode for the three PC/NG discharge cases. At some time during the discharge the electric field drops from $E \approx 4$ V/cm to < 0.3 V/cm over a ≈ 30 μ s timescale. This represents a time when the beam range just equals the distance from cathode to the probe location. The average neutral gas density upstream of the probe location may be calculated by taking a line integral of the energy loss given by equation (2) from its initial energy to zero. This gives

$$R = 2.08 \times 10^{-6} \left(\frac{W^2}{P_N} \right) \quad [cm] \quad (7)$$

for the beam range where W is the electron energy and P_N is the average pressure of the gas along the electron path. Early in the pulse ($t \approx 20$ μ s), when the pressure is still $P_N \approx 208$ mTorr, the cathode voltages for the three cases shown in figure 3 were $V_c \approx 0.9, 1.0$, and 1.1 kV for the $V_0 = 2.0, 2.5$, and 3.0 cases respectively. From equation (7) the range of the highest energy electrons ($W = V_c$) is $8.1, 10.0$, and 12.1 cm respectively, well short of the 35 cm probe location. Thus early in time one would not expect the beam electrons to reach the probe. From figure 6 the transitions from the high electric field PC discharge to the NG discharge occur at approximately $155, 115$, and 95 μ s respectively. Figure 3a gives the cathode voltages at these times to be $1.18, 1.35$, and 1.45 kV. Assuming the range at these times is 35 cm, equation (7) gives average pressures between the cathode and the probe of $83, 108$, and 125 mTorr for the three cases. This compares well with the pressures derived in section V.C of $93, 121$, and 129 mTorr using electric field measurements in the PC just before transition.

Additional evidence that the beam range and the transition time are linked comes from spectral measurements. In figure 4 the 4597 Å spectral line shows a peak at $t = 140 \mu s$. The field of view of the spectrometer was approximately 42 cm from the cathode on this shot. This is consistent with the transition time for the discharge and most likely represents the beam range sweeping past the field of view of the spectrometer. Early in time, when the field of view is in the PC portion of the discharge, this line intensity is small. Later, after the NG covers the entire discharge region, it is large. As the beam sweeps past, a 30 μs FWHM peak shows up.

F. Self-consistent Calculation of Channel Density

A self-consistent model of the discharge can be derived using the plasma continuity equation and experimental measurements of V_D , I_D and E . As discussed above there are two modes of operation for the discharge, NG and PC, corresponding to two separate sources of ionization. In the low temperature, high plasma density NG mode the plasma is generated by beam induced ionization. In the higher temperature, low plasma density PC mode the plasma is produced by avalanche ionization. Important loss mechanisms in both types of discharge include two-body recombination and ambipolar diffusion. Equations for the production and loss of plasma combined with experimental measurements may be solved to obtain a self-consistent set of equations describing the evolution of the plasma. Solutions for the neutral gas density and other plasma parameters can then be compared with other independent experimental measurements.

The rate of particle production due to beam induced ionization in the NG is given by Eq. (3). Note that this assumes a mono-energetic electron beam. In general, the average energy lost per electron-ion pair produced in a plasma discharge is much greater (by a factor of 10^3 - 10^4) than the ionization energy, W_{ion} , due to collisional losses to the background gas. For cases where the ionizing particle has energy $W \gg W_{ion} \approx 15$ eV the average drops to $W_L \approx 2 W_{ion}$.

In the PC, plasma is produced by avalanche ionization at a rate given by

$$\left. \frac{\partial n_e}{\partial t} \right|_{aval} = v_{iz} n_e \quad (8)$$

where v_{iz} can be expressed⁵ as the neutral gas density N times a function of the reduced electric field, E/N . In air, this rate is non-zero only if $E/N \geq 10^{-15}$ V-cm². In the density regime at which the PC/NG discharge operates losses due to recombination and transverse diffusion are both important. Recombination losses are given by Eq. (4). The recombination coefficient, $\beta \approx 5 \times 10^{-8}$ cm³/s, independent of the neutral density. Diffusion losses are estimated by

$$\left. \frac{\partial n_e}{\partial t} \right|_{diff} \equiv D_a \nabla^2 n_e \equiv -D_a \frac{n_e}{\Delta x^2}, \quad (9)$$

where Δx is the characteristic half-width of the plasma sheet, D_a is the ambipolar diffusion coefficient,

$$D_a \equiv \frac{k(T_e + T_i)}{m_e v_{em} \left[1 + (\omega_{ce}/v_{em})^2 \right] + M_i v_{im}}, \quad (10)$$

T_e and T_i are temperatures in °K, k is the Boltzman constant, ω_{ce} is the electron-cyclotron frequency, and v_{em} and v_{im} are the electron and ion momentum collision frequencies. Here the massive ions are treated as unmagnetized. The ionization and loss processes balance in steady state, so that

$$\frac{j_b}{e} \frac{1}{W_{ei}} \left(\frac{\partial W}{\partial z} \right) + v_{iz} n_e - \beta n_e^2 - e D_a \nabla^2 n_e = 0. \quad (11)$$

The parameters v_{iz} , β_r , and D_a may be specified as functions the electric field $E(t,z)$ and neutral gas density $N(t)$ using swarm data.⁶ The discharge current is given by $I_D(t) = e A n_e v_d$, where A is the discharge cross sectional area and $v_d(E/N)$ is the average electron drift velocity, found in swarm tables⁶ for the appropriate gas species. Eq. (11) is then be expressed entirely in terms of experimentally measured quantities and parameters that are known functions of E/N , except for the beam current j_b . Substituting $j_b \approx \gamma_d \cdot j_d = \gamma_d \cdot e v_d n_e$ and $I_D = e A v_d n_e$, Eq. (11) becomes

$$e A v_d \left\{ C \frac{\gamma_d v_d}{W_{ei}} \frac{Z N(t)}{W} \left[\ln \left(\frac{W}{P} \right) + 0.15 \right] + v_{iz} - \frac{D_a}{\Delta x^2} \right\} - \beta I_D(t) = 0. \quad (12)$$

Here $C = 1.3 \times 10^{-13}$, $\gamma_d = \gamma_{\text{eff}} / (1 + \gamma_{\text{eff}}) \approx \gamma_{\text{eff}}$ for the discharges of interest, and $P = 88$ eV is related to the impact parameter for high energy electrons ionizing air.

Substituting measured values of $E(t)$, $I_D(t)$, $W(t)$ into Eq. (12) and solving numerically yielded values for $N(t)$, $n_e(t)$, γ_{eff} , and $T_e(t)$ which could be compared with independent experimental measurements. An example of the results for $z = 35$ cm is shown in Fig. 10. This location was well within the PC portion of the discharge early in time. The initial neutral density is $N(0) = 7.4 \times 10^{15} \text{ cm}^{-3}$ equals the neutral gas density of room temperature air at $P_N = 208$ mTorr. Equation (12) shows that $N(t)$ drops by $\sim 50\%$ during the PC phase of the discharge and levels off late in time during the NG phase. The numerical solution failed to converge during the transition period from $75 < t < 140 \mu\text{s}$ when the beam is passing the probe location. A more complete model of the electron beam including the effects of finite beam energy spread would be required to obtain a physical solution in this regime.

The electron density calculated via Eq. (12) indicates that $n_e \approx 9 \times 10^{10} \text{ cm}^{-3}$ for $t > 125 \mu\text{s}$, and somewhat lower earlier. Electron temperatures, which are a function of E/N for the discharge, were nearly constant at $T_e \approx 2 - 2.5$ eV during the PC phase of the discharge pulse. Later in time, during the NG phase, T_e drops to $T_e \approx 0.9$ eV. Langmuir probe measurements yield $T_e \approx 3.0$ eV and 1.2 eV respectively in the PC and NG in reasonably good agreement with the numerical solution.

VI. Conclusions

Measurement of a negative glow discharge produced using a hollow cathode yielded a plasma with density $n_e \approx 10^{12} \text{ cm}^{-3}$, electron temperature $T_e = 1$ eV, and electric field $E = 0.1$ V/cm for a power supply voltage of $V_0 = 6.5$ kV, magnetic field $B = 250$ G and air pressure of $P_N = 120$ mTorr. For $P_N = 208$ mTorr, $V_0 = 2-3$ kV, and $B = 250$ Gauss the discharge displayed separate and distinct positive column and negative glow regions early in time. In this case Langmuir probe measurements indicated that $E \approx 6-8$ V/cm in the PC and $n_e \approx 8.5 \times 10^{10} \text{ cm}^{-3}$, $T_e \approx 1.1$ eV, and $E \approx 0.35$ V/cm in the NG. The plasma in the NG region of both discharges is produced by a high energy electron beam emitted from the hollow cathode, while the plasma in the PC region is

sustained by avalanche ionization. Later in time, over a 150 μ s time scale, the PC/NG discharge was observed to transition from an initially stable NG/Faraday Dark Space/PC configuration to a single NG region. The time of transition was consistent and highly repeatable. Floating probe measurements verified that the electric field in the PC region of the 300 μ s long discharge pulse decayed from an initial 8 V/cm to a final 0.3 V/cm, indicating that a supplemental source was contributing to ionization within the PC region as time progressed. This was confirmed by spectral and electric probe diagnostics, which showed evidence of kilovolt electrons late in time. A numerical solution of the electron continuity equation employing electron swarm data relationships and time resolved measurements of the electric field, discharge current, and discharge voltage gave $n_e(t)$, $T_e(t)$, and $N(t)$ in the discharge channel. These calculations indicate that $N(t)$ decreased by $\approx 50\%$ after $\approx 150 \mu$ s. Energy exchange calculations indicate that this reduction is consistent with discharge heating of the neutral background gas within the channel. As $N(t)$ decreased, the cathode-produced electron beam range increased and the primary ionization source within the PC region transitioned from avalanche ionization to beam ionization. Similar heating within the cathode fall region changed the operating characteristics of the hollow cathode itself. There are indications of this in the discharge impedance which increased by an order of magnitude over a 150 μ s time scale. Additionally, the effective secondary emission coefficient is seen to vary by an order of magnitude between the NG-only and PC/NG discharges, due primarily to the difference in neutral gas density within the hollow cathode region in these two cases. These effects are consistent with a significant reduction in neutral gas density within the cathode fall region, resulting in an increased cathode fall length.

Acknowledgements

Work supported by the Office of Naval Research. Dr. W. Manheimer provided theoretical support and Drs. J. Mathew, R. E. Pechacek, and D. P. Murphy provided assistance in the design, construction, and fielding of the diagnostics used for this experiment. M. C. Myers and A. Knoll for provided engineering and technical support for this work.

References

¹W. M. Manheimer, IEEE Trans. on Plasma Sci. 19 (6), 1228-1234 (1991)

²A. E. Robson, R. L. Morgan, and R. A. Meger, IEEE Trans. Plasma Sci. 20 (6), 1036-1040 (1992).

³R.A. Meger, J. Mathew, J. A. Gregor, R. E. Pechacek, R. F. Farnsler, W. Manheimer, A. E. Robson, Phys. Plasmas 2 (6), 2532-2538, (1995).

⁴J. Mathew, R. F. Farnsler, R. A. Meger, J. A. Gregor, D. P. Murphy, R. E. Pechacek, W. M. Manheimer, Phys. Rev. Lett. 77(10), 1982-1985 (1996).

⁵R. F. Farnsler, W. M. Manheimer, R. A. Meger, J. Mathew, D. P. Murphy, R. E. Pechacek, J. A. Gregor, Physics of Plasmas 5(5), 2137 (1998).

⁶Dutton, J. Physics Chemical Reference Data 4(3), 578-777 (1975).

⁷Y. P. Raizer, Gas Discharge Physics (Springer-Verlag, Berlin, 1991), p. 338-341.

⁸J. Mathew, Rev. Sci. Instrum. 65 (12), 3756-3760 (1994).

⁹J. Mathew, R. A. Meger, R. F. Farnsler, J. A. Gregor, Rev. Sci. Instrum. 67(8), p. 2818-2825 (1996).

¹⁰R. A. Meger, J. A. Gregor, R.F. Farnsler, W.M. Manheimer, J. Mathew, M.C. Myers, R.E. Pechacek, IEEE Trans. Plasma Science 27(1), p. 1000 (1999).

¹¹Y. P. Raizer, Gas Discharge Physics (Springer-Verlag, Berlin, 1991), p. 171.

¹²J. D. Jackson, Classical Electrodynamics (John Wiley & Sons, Inc., New York, 1962), p.434.

¹³F. J. Mehr, M. A. Biondi, Phys. Rev. 181, p. 264-270 (1969).

¹⁴Y. P. Raizer, Gas Discharge Physics (Springer-Verlag, Berlin, 1991), p. 71.

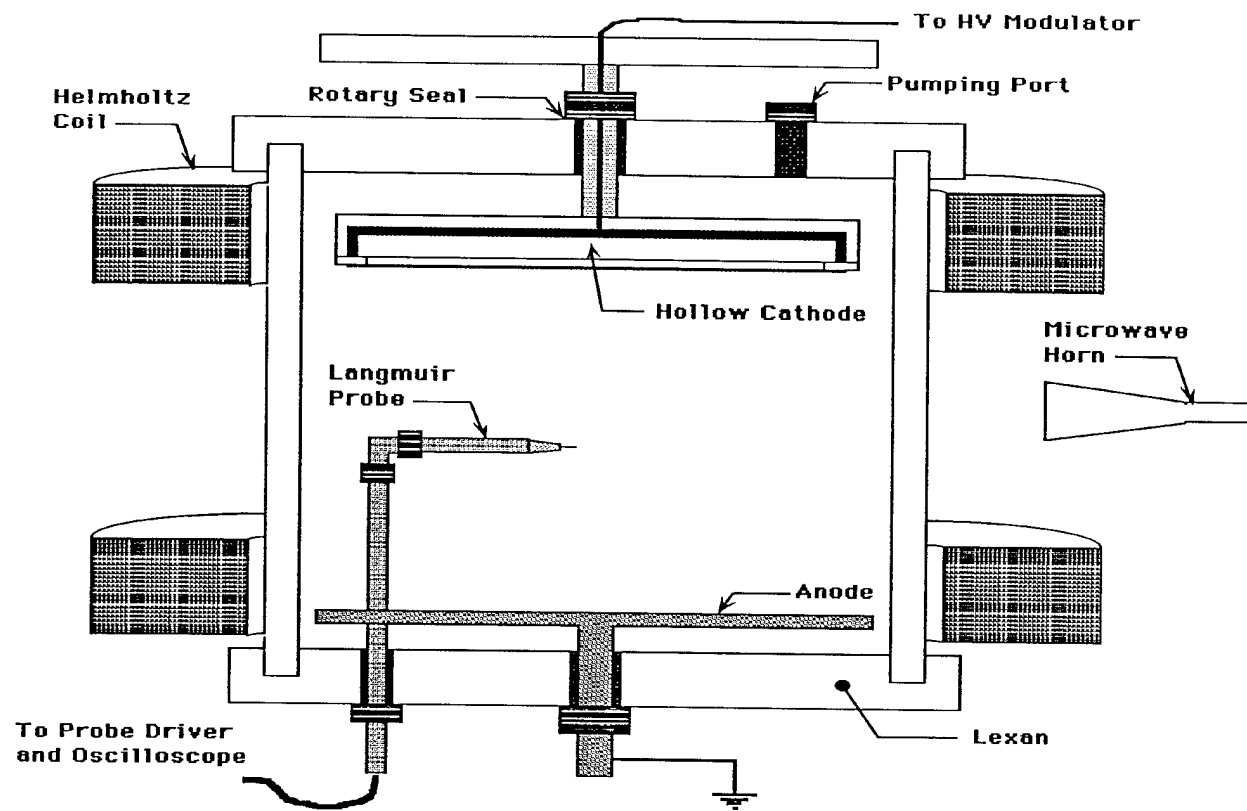


Figure 1. Schematic of the Agile Mirror system with diagnostics shown.

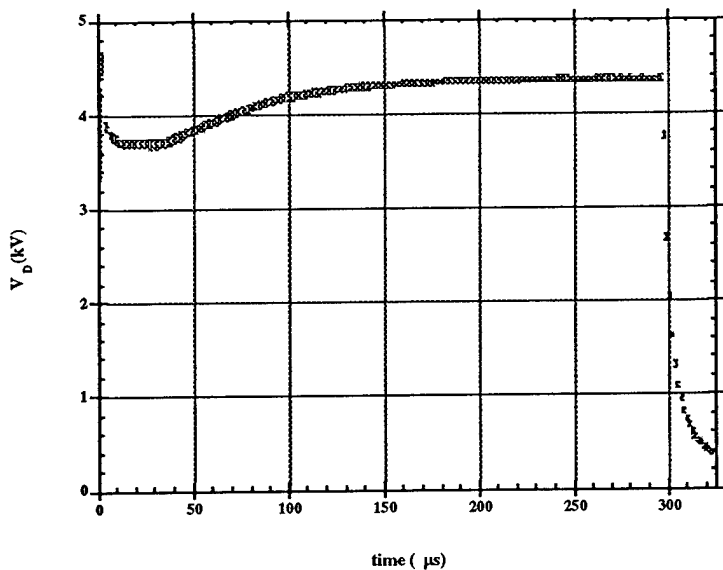


Figure 2a. Voltage for NG-only case with $V_0 = 6.5$ kV, $P_N = 120$ mTorr, and $B = 250$ G.

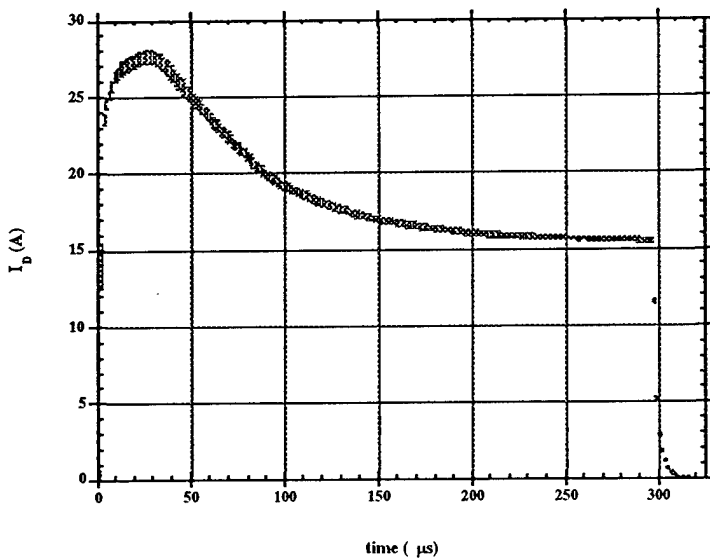


Figure 2b. Current for NG-only case.

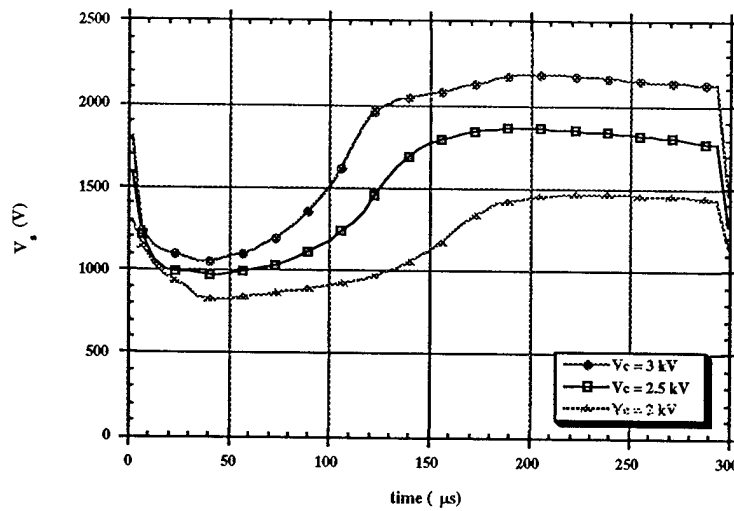


Figure 3a. Voltage for PC/NG cases with, $V_0 = 2, 2.5$, and 3 kV, $P_N = 208$ mTorr, and $B = 250$ G.

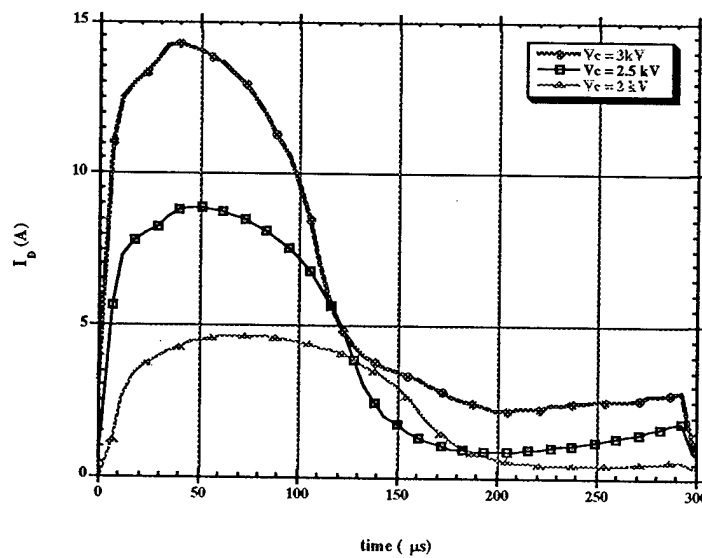


Figure 3b. Current for PC/NG cases.

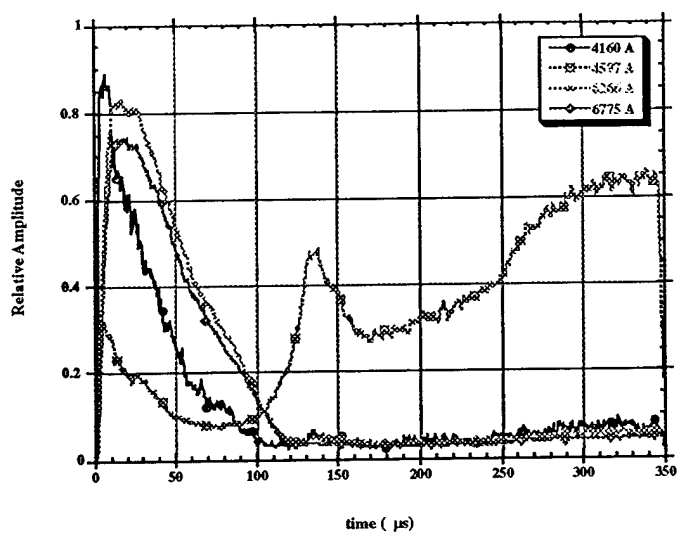


Figure 4. Optical emissions from the PC/NG $V_0 = 3$ kV discharge at the $z = 42$ cm.

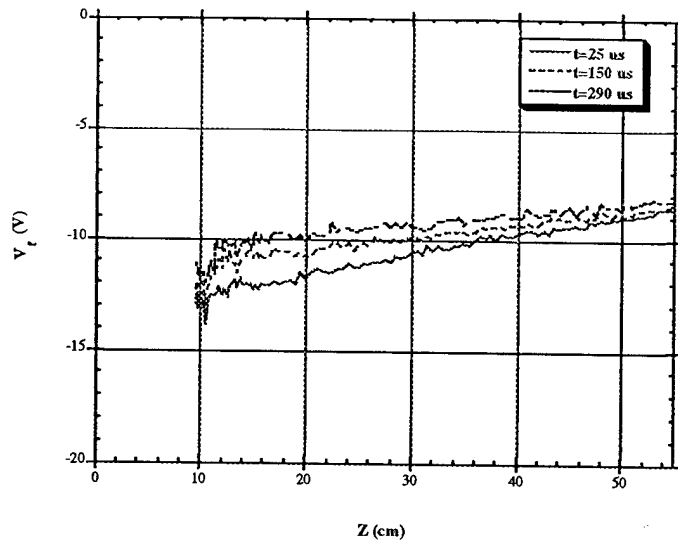


Figure 5a. Measured floating potential the NG-only case at 25, 150 and 290 μ s.

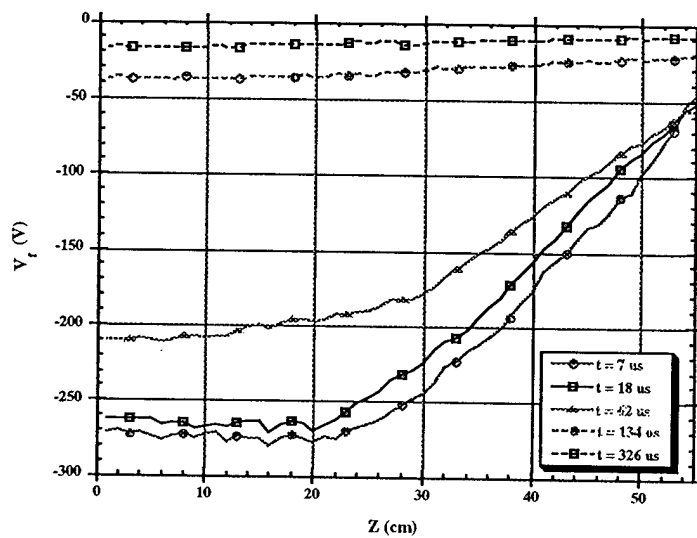


Figure 5b. Floating potential for the PC/NG discharge with $V_0 = 3$ kV.

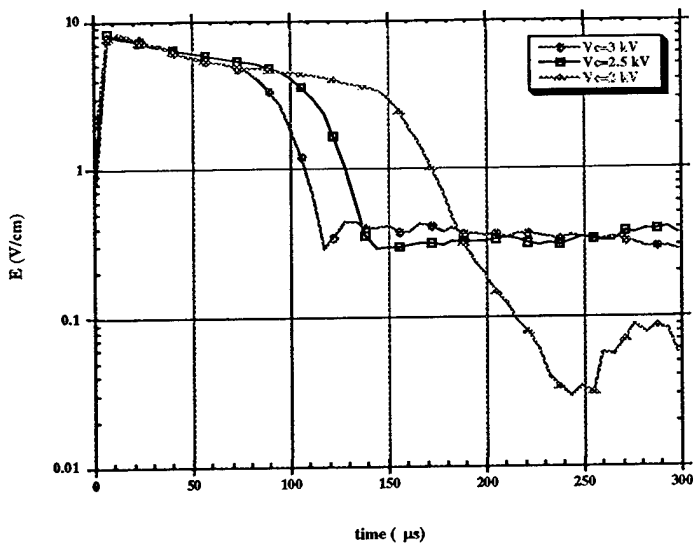


Figure 6. Electric field in the PC/NG discharge at $z = 35$ cm and $V_0 = 2.0$, 2.5, and 3.0 kV.

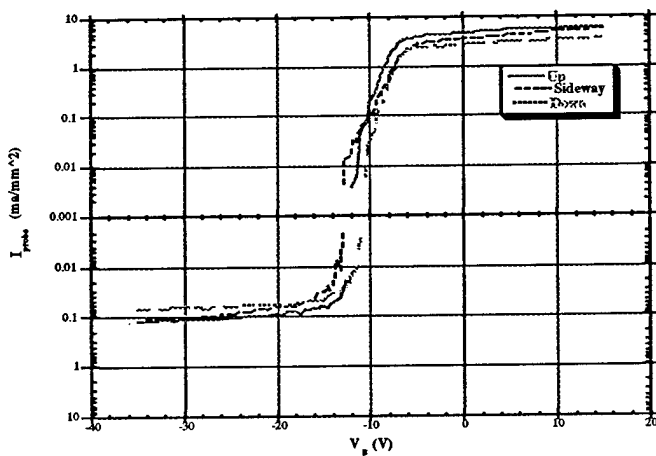


Figure 7. Langmuir probe characteristic curves for the NG-only case. Probe oriented facing up, down, and sideways with respect to the cathode-anode axis.

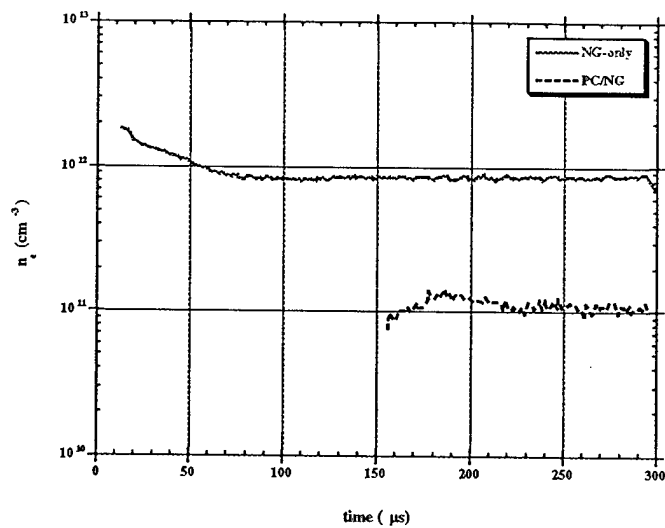


Figure 8. Electron density for the NG-only and the 3 kV PC/NG case.

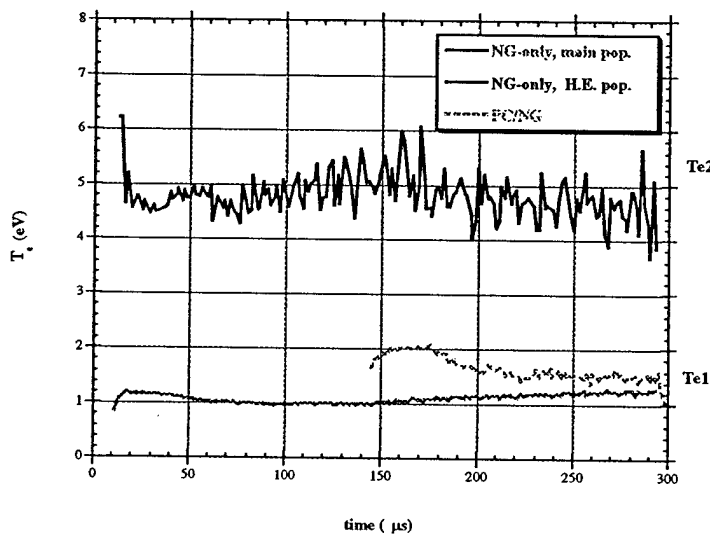


Figure 9. Electron temperature for NG-only and the $V_0 = 3$ kV PC/NG case.

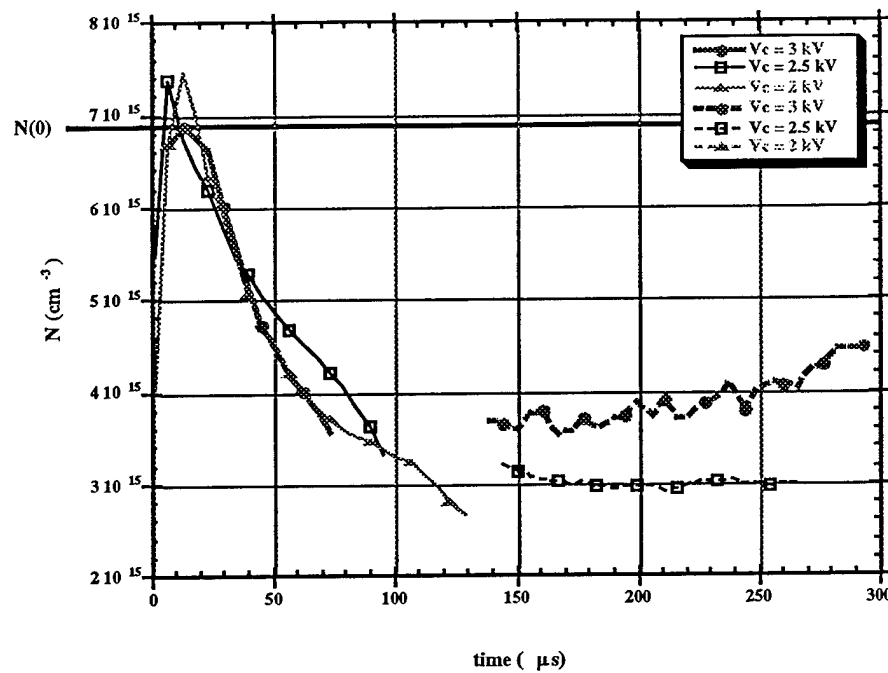


Figure 10. Calculated neutral gas density in the PC/NG discharge 35 cm downstream from the cathode for the $V_0 = 2, 2.5$, and 3 kV cases. Solid lines indicate PC phase and dashed lines indicate NG phase.